https://doi.org/10.5194/egusphere-2025-6288
Preprint. Discussion started: 19 December 2025

Natural disturbances increasingly affect Europe's most mature and carbon-rich forests

Simon Besnard[1], Alba Viana-Soto[2], Henrik Hartmann[3,4,5], Marco Patacca[6,7], Viola H.A. Heinrich[1,8], Katja Kowalski[2], Maurizio Santoro[9], Wanda De Keersmaecker[10], Ruben Van De Kerchove[10], Martin Herold[1], Cornelius Senf[2]

[1]GFZ Helmholtz Centre for Geosciences, Telegrafenberg, 14473 Potsdam, Germany

[2]Technical University of Munich, School of Life Sciences, Earth Observation for Ecosystem Management, Freising, Germany

[3]Julius Kühn Institute (JKI) - Federal Research Centre for Cultivated Plants, Institute for Forest Protection, Quedlinburg, Germany.

[4]Faculty of Forest Sciences and Forest Ecology, Georg-August-University, Büsgenweg 5, 37077 Göttingen, Germany

[5]Department of Biogeochemical Processes, Max Planck Institute for Biogeochemistry, Hans Knoell Str. 10, 07745 Jena, Germany

[6]Sustainable Forest Ecosystems, Wageningen Environmental Research, Wageningen, The Netherlands

[7]Forest Ecology and Forest Management Group, Wageningen University and Research, Wageningen, The Netherlands

[8]School of Geographical Sciences, University of Bristol, Bristol, United Kingdom

[9]Gamma Remote Sensing, 3073 Gümligen, Switzerland

[10]Environmental Intelligence, Flemish Institute for Technological Research (VITO), Mol, Belgium

Correspondence to: Simon Besnard (simon.besnard@gfz.de)

Abstract. Europe's forests store nearly 40 PgC and provide a critical carbon sink of ~0.2 PgC yr^{-1}, yet climate-driven disturbances increasingly threaten this capacity. Although disturbance rates from windthrow and bark beetle outbreaks have risen in recent decades, it remains unclear whether these events increasingly affect the oldest and largest trees, which store a disproportionate share of carbon. Here, we combine three decades of satellite-derived disturbance maps with spatially explicit data on forest age, biomass, and species composition to reveal patterns of structural selectivity across Europe. We show that natural disturbances have shifted toward older, carbon-rich stands, with disturbed forest area>60 years old nearly tripling since 2010 (from 0.38 to 1.06 Mha). This structural shift is most pronounced in spruce-dominated regions of Central Europe (effect size = 1), where compound heat and drought events have amplified susceptibility to bark beetles. Biomass losses from natural disturbances in spruce forests increased eightfold between the early (2011-2016) and recent (2017-2023) periods. Trend-based projections indicate that, if current patterns of structural selectivity persist, natural disturbances could expose biomass carbon stocks equivalent to approximately 20% of Europe's contemporary forest carbon sink by 2040 (~0.05 PgC yr^{-1} or ~0.7 PgC cumulative). Our findings reveal a previously unquantified vulnerability: climate-driven disturbances increasingly affect forest structures with high per-hectare carbon stocks, amplifying disturbance-related carbon exposure and weakening the long-term effectiveness of Europe's forest carbon sink. Adaptive management strategies that promote

https://doi.org/10.5194/egusphere-2025-6288
Preprint. Discussion started: 19 December 2025

structural and compositional diversification in high-risk regions will be critical to stabilise forest carbon storage under continued climate change.

1 Introduction

European forests are central to the continent's climate mitigation efforts, storing nearly 40 PgC in aboveground and soil carbon pools and acting as a net carbon sink of ~0.2 PgC per year between 2010 and 2019 (Pan et al., 2024). Yet, this sink is weakening. A large share of Europe's forests originated from post-war planting campaigns and are entering maturity, during which carbon accumulation slows as stands approach saturation (Nabuurs et al., 2013). At the same time, harvest levels have remained high or increased in recent decades (Turubanova et al., 2023), and climate-sensitive natural disturbances (e.g., windthrow and bark beetle outbreaks) are intensifying across the region (Seidl and Senf, 2024). These pressures are particularly concerning for structurally mature forests dominated by large, old trees, which store a disproportionate share of carbon and sustain long-term sequestration (Besnard et al., 2025).

We define disturbances broadly as either natural or anthropogenic in origin. Natural disturbances are events triggered by environmental agents such as windstorms and bark beetle outbreaks (including associated salvage logging), whereas harvest refers to timber removal directly driven by management. Natural disturbances have become more frequent and severe in recent decades (Patacca et al., 2023), coinciding with reports of declining forest carbon sinks in parts of Europe (Migliavacca et al., 2025; Ritter et al., 2025). Since 2018, bark beetle outbreaks have surpassed windthrow as the dominant natural cause of canopy loss (Patacca et al., 2023) (Fig. S1), especially in Central Europe (Austria, Germany, Czechia, and parts of northern Italy), where compound droughts and heatwaves have predisposed spruce to infestation, resulting in unprecedented mortality ("Living with bark beetles," 2019; Weynants et al., 2024). Warming further accelerates bark beetle reproduction (Wermelinger and Seifert, 1999), enabling multiple generations per year (Jakoby et al., 2019) and facilitating outbreaks at higher elevations (Hartmann et al., 2025) and more northerly latitudes ("Korhonen K. T., Ahola A. et al. (2021) Forests of Finland 2014-2018 and their development 1921-2018," n.d.; "Pulgarin Diaz J. A., Melin M. et al. (2024) Relationship between stand and landscape attributes and *Ips typographus* salvage loggings in Finland," n.d.). These trends are likely to continue as climate change continues. Although beetles dominate today, periodic windstorms have historically caused catastrophic losses, and future storms could again shift disturbance dynamics, as seen with events such as Vivian and Wiebke (1990), Lothar and Martin (1999), and Klaus (2009).

Despite extensive documentation of disturbance extent and trends across Europe (Ceccherini et al., 2020; Hansen et al., 2013; Turubanova et al., 2023; Viana-Soto and Senf, 2025) (Fig. S2), the structural characteristics of affected forests, especially their age and biomass, remain poorly quantified at a continental scale. Local studies suggest that older, high-biomass stands may be particularly vulnerable to natural disturbances (Brockerhoff et al., 2008; Jactel et al., 2017; Neuner et al., 2015); yet it remains unclear whether disturbances show systematic structural selectivity at continental scales.

https://doi.org/10.5194/egusphere-2025-6288
Preprint. Discussion started: 19 December 2025

Susceptibility likely depends on both species composition and structural heterogeneity, with homogeneous stands offering continuous host connectivity that facilitates the spread of disturbance (Raffa et al., 2008). The critical question is whether rising disturbance rates are driven primarily by expanding spatial footprints or by a systematic shift toward structurally vulnerable cohorts, and how this selectivity may reshape Europe's forest carbon dynamics. Answering this is essential not only for anticipating demographic and carbon trajectories but also for improving Earth system models, which often represent disturbances stochastically or without structural constraints (Bergkvist et al., 2025; Calle and Poulter, 2021; O'Sullivan et al., 2024).

Here, we present the first continental assessment of structural and compositional selectivity in recent forest disturbances across Europe. We examine whether disturbance impacts have shifted toward older, carbon-rich stands and how these patterns vary across dominant genera. Integrating three decades of satellite-derived disturbance maps (Viana-Soto and Senf, 2025) with spatially explicit forest age (Besnard et al., 2021, n.d.), aboveground biomass (Santoro and Cartus, 2023), and genus composition (De Keersmaecker et al., 2024), we ask whether natural disturbances are increasingly affecting older, carbon-dense forests. We quantify shifts in the age and biomass structure of disturbed stands, test whether impacts concentrate in structurally homogeneous forests, and project how continued structural selectivity may increase the exposure of forest carbon stocks to disturbance through 2040. Our findings indicate that Europe's forest carbon sink is becoming increasingly vulnerable not only because disturbance rates are rising, but also because disturbances are disproportionately affecting forest areas with high carbon stocks.

2 Materials and Methods

2.1 Annual disturbance data resampling

To generate spatially consistent disturbance layers across Europe, we resampled annual disturbance maps from the European Forest Disturbance Atlas v2.1.1 dataset (Viana-Soto and Senf, 2025) to a 100 m grid (EPSG: 4326) aligned with the ESA CCI biomass dataset (Santoro and Cartus, 2023). EFDA provides annual maps indicating, for each 30 m pixel, whether a disturbance occurred (binary 0/1) and the associated agent (harvest, wind/bark beetle, fire, mixed).

We first reprojected each annual EFDA layer to EPSG:4326. The reprojected 30 m binary maps were then aggregated to 100 m resolution using average resampling, which converts the number of disturbed 30 m sub-pixels within each 100 m cell into a disturbance fraction. This approach preserves information on sub-pixel heterogeneity and yields, for each 100 m pixel, the proportion of forested area disturbed by a given agent in a given year.

To account for known commission errors (Viana-Soto and Senf, 2025) in the disturbance maps for 2018 and 2023 over northern latitudes, we excluded all disturbance values for these two years in areas north of 65°N. This filtering step mitigates the influence of artefact-driven expansions in the boreal region. Fire and mixed disturbances were excluded from this study.

https://doi.org/10.5194/egusphere-2025-6288
Preprint. Discussion started: 19 December 2025

We focus on two disturbance types: harvest, representing human forest management activities, and wind/bark beetle, representing natural disturbances driven by natural factors.

The final dataset consists of harmonised, agent-specific disturbance-fraction layers at 100 m resolution for the period 1985-2023. These layers are spatially aligned with the forest age and biomass products used in downstream analyses, ensuring consistent pixel-level integration across all data streams.

2.2 Genus map data resampling

To incorporate tree species composition into the analysis, we downscaled the 10 m European genus classification map (De Keersmaecker et al., 2024) (EPSG:3035) to a 100 m grid in EPSG:4326, ensuring consistency with the forest age, biomass, and disturbance datasets. The map distinguishes eight classes: Larix, Picea, Pinus, Fagus, Quercus, other needleleaf, other broadleaf, and no-tree. The 10 m genus labels were first reprojected to EPSG:4326. We then aggregated the reprojected map to 100 m resolution using a mode-based majority filter, assigning each 100 m cell the genus class that occurred most frequently among its underlying 10 m pixels.

This procedure preserves the dominant-genus signal while reducing spatial detail to the scale of the biomass-product and disturbance layers. The resulting 100 m genus map is fully aligned with the European forest domain and all other gridded datasets used in subsequent analyses.

2.3 Integration of the different Earth Observation data streams

To build a unified dataset for analysis, we first identified all forested pixels that experienced either harvest or natural disturbances (windthrow or bark beetle) between 1985 and 2023, as mapped in the European Forest Disturbance Atlas v2.1.1. For every disturbed 100 m pixel (in EPSG:4326), we extracted co-located forest structural and compositional attributes.

Each disturbed pixel was associated with:

1. The annual disturbance fraction for each agent (harvest, natural disturbance),
2. forest age from the GAMI v3.0 ensemble (Besnard et al., 2021, n.d.) (20 members),
3. aboveground biomass from the ESA CCI biomass v6.0 ensemble (20 members; converted to carbon),
4. forest fraction at 100 m, and
5. the dominant genus class (resampled from the 10 m genus map).

https://doi.org/10.5194/egusphere-2025-6288
Preprint. Discussion started: 19 December 2025

The resulting dataset is stored in tabular format, with each row corresponding to a single forested pixel that was disturbed at least once between 1985 and 2023.

2.4 Integration of the different Earth Observation data streams

To assess whether the age structure of disturbed forests changed over time, we examined shifts in the 2010 baseline forest age of pixels affected by harvest or natural disturbances. Using the harmonised disturbance dataset (2011-2023), we selected all 100 m pixels with ≥30% forest fraction. We retained only those where ≥50% of the forested area was disturbed by a specific agent in a given year. Forest age was obtained from the 20-member GAMIv3.0 ensemble, and we used the 2010 age estimate for all years to remove the confounding effect of natural forest ageing.

We aggregated all pixel-level information onto a 100 km-diameter hexagonal grid to increase robustness in regional comparisons. For each hexagon and disturbance type, we calculated the median 2010 age of disturbed pixels for the early (2011-2016) and recent (2017-2023) periods. Differences between periods indicate whether disturbances increasingly affected older or younger forests, independent of stand development.

To quantify changes in the full age distribution, we used the energy distance (ED) metric (Rizzo and Székely, 2016), which measures divergence between two probability distributions and is sensitive to both shifts in central tendency and distributional shape. ED between the early and recent periods was computed for each hexagon and disturbance type:

$$ED(X, Y) = 2 * E[||X - Y||] - E[||X - X'||] - E[||Y - Y'||] \quad \text{Eq. (1)}$$

Where X and Y represent the 2010 age distributions of disturbed pixels in the early and recent periods, X′ and Y′ are independent copies of X and Y, and $\|\cdot\|$ denotes the Euclidean distance.

To complement age-based analyses, we evaluated how the joint distribution of forest age and aboveground biomass (AGB) changed across disturbance types and periods. Disturbed pixels were binned into a 7×7 matrix of age and biomass classes for each period (e.g. 0-20, 21-40, ..., >120 years or MgC ha^{-1}), and the fraction of pixels in each structural class was computed to form two-dimensional disturbance density matrices. Matrix differences (recent minus early) highlight which structural cohorts gained or lost prominence in recent disturbances.

Given known ecological thresholds (e.g., bark beetles preferentially affecting spruce > ~60 years) (Hlásny et al., 2021), we further grouped stands into broad age classes (1-60 years, > 60 years) and computed annual fractions disturbed in each class. For all metrics, we summarised uncertainty across the 20-member ensembles using medians and 5th-95th percentiles. Temporal trajectories were visualised separately for natural disturbances and harvests. These analyses enabled us to

https://doi.org/10.5194/egusphere-2025-6288
Preprint. Discussion started: 19 December 2025

145 determine whether disturbances increasingly targeted older and/or higher-biomass stands, and whether these structural shifts differed between natural disturbances and harvest activities.

2.5 Species-specific biomass loss assessment

To investigate species-specific susceptibility to disturbance, we assessed the structural and cumulative biomass loss across three genus groups: Spruce, Other needleleaf (including *Larix*, *Pinus*, and other conifers), and Broadleaf (including *Fagus*,
150 *Quercus*, and other broadleaf species). The analysis focused on harvests and natural disturbances (wind and bark beetles) across two periods: 2011-2016 and 2017-2023. For each disturbed pixel, we used ensemble median aboveground biomass estimates (converted to carbon using a factor of 0.47), forest fraction, genus class, and disturbance fraction. Biomass values were filtered to remove non-positive and extreme outliers (IQR-based filtering). Cohen's d effect sizes were calculated to quantify shifts in biomass distribution between early and recent periods within each genus group. To assess total biomass
155 loss, we aggregated disturbed biomass by multiplying per-pixel biomass by forest fraction, pixel area, and disturbance fraction, and then summing across all pixels within each genus and period. This was repeated across 20 biomass members to derive ensemble medians and uncertainty bounds (5^{th}-95^{th} percentiles). The resulting values were expressed in terragrams of carbon (TgC). Together, these analyses provide a quantitative view of how biomass loss from disturbances varies by species group and whether structural shifts or total loss intensified in the more recent period.

160 ### 2.6 Assessing structural homogeneity in disturbed forests

To determine whether natural disturbances increasingly affect structurally homogeneous forest stands, we quantified spatial and temporal changes in structural variability using the coefficient of variation (CV) of aboveground biomass (MgC ha^{-1}). Biomass CV was calculated as a proxy for stand-level structural heterogeneity.

We used harmonised disturbance and biomass datasets at 100 m resolution across Europe from 2011 to 2023, covering both
165 natural disturbances (windthrow and bark beetle) and harvests. All data were aggregated to a 100 km hexagonal grid (EPSG:3035) to ensure consistency in regional comparisons. Pixels were included if forest cover exceeded 30%, and disturbance affected more than 50% of the forested area in a given year. For each hexagon, CV values were computed separately for each member of the 20-realisation biomass ensemble; hexagons with fewer than 50 valid disturbed pixels were excluded.

170 Structural heterogeneity was compared between early (2011-2016) and recent (2017-2023) disturbance periods. Analyses were stratified by disturbance type and by forest genus (spruce, other needleleaf, broadleaf). Differences between periods were quantified using Cohen's *d* and mapped as ΔCV (recent minus early). To assess continuous shifts, we calculated the annual median CV for each ensemble member and aggregated these across the 20 biomass realisations. For each disturbance

https://doi.org/10.5194/egusphere-2025-6288
Preprint. Discussion started: 19 December 2025

type and genus, we fitted ordinary least-squares regressions of CV against year; slopes and significance levels summarised long-term changes in structural heterogeneity. Temporal coherence between harvest- and disturbance-related CV trajectories was evaluated using Pearson's *r*.

2.7 Trend-based forecasts of biomass exposure through 2040

Spatial aggregation and disturbance quantification: We used annual disturbance and biomass datasets at 100 m resolution across Europe (1985-2023), covering both natural disturbances (windthrow, bark beetle) and harvest. Disturbance metrics were aggregated to a 100 km hexagonal grid to enable robust regional trend analysis. Pixels were retained if forest cover exceeded 30%, and, within these, if more than 50% of the forested area was disturbed by a given agent in a given year. Hexagons with fewer than 50 valid pixels were excluded. This filtering captures high-severity, stand-replacing events, where most of the canopy is affected, and therefore produces conservative disturbance estimates that underrepresent low-severity or partial disturbances. Aboveground biomass values from the ESA CCI v6.0 ensemble (20 realisations) were converted to carbon using a factor of 0.47. Median biomass per hexagon, disturbance type, and period was used in subsequent simulations.

Annual disturbed area and biomass exposure: For each disturbance type and year, we computed the total disturbed forest area per hexagon as:

$$A_{i,y} = f_{i,y} * d_{i,y} * a_i \quad \text{Eq. (2)}$$

Where $f_{i,y}$ is the forest fraction in pixel i and year y, $d_{i,y}$ is the disturbance fraction in pixel i and year y, and a_i is the area of pixel i (converted to Mha). The total disturbed area for each year and disturbance agent was obtained by summing $A_{i,y}$ across all pixels within a hexagon. This produced an annual time series of total disturbed area per hexagon from 1985 to 2023, which was used as input for forecasting.

Trend-based forecasting and model selection: To reduce short-term noise, annual disturbance trajectories were smoothed using a centred 5-year moving average. Model fitting was restricted to recent periods (2008-2023, or 2015-2023 in sensitivity tests) to capture contemporary disturbance dynamics. For each hexagon and disturbance agent, we fit two candidate models to the smoothed series: (i) linear increase and (ii) exponential decay, and selected the best model using the Akaike Information Criterion (AIC). Decay models were constrained to plausible decreasing trends, reflecting potential stabilisation after outbreak peaks. Linear models represented continued intensification. The selected model was then used to forecast areas of disturbance for 2024-2040.

https://doi.org/10.5194/egusphere-2025-6288
Preprint. Discussion started: 19 December 2025

Uncertainty estimation via Taylor's law: To account for heteroskedasticity in disturbance dynamics, we applied Taylor's law (Taylor, 1961) separately to natural disturbances and harvest. For each hexagon, we computed the mean and variance of annual disturbed area over the model-fitting window (2008-2023; or 2015-2023 in sensitivity tests). These mean-variance pairs were then pooled across all hexagons and fit with a log-log linear regression, yielding global parameters *a* and *b*:

$$Var(A_y) = a * \mu_y^b \quad \text{Eq. (3)}$$

Where $Var(A_y)$ is the variance of the annual disturbed area in year y, μ_y is the mean yearly disturbed area in year y, and a and b are regression parameters estimated from historical data. Projected variances for 2024-2040 were derived using the predicted means and this relationship.

Mean-variance pairs were then reparameterised into lognormal distributions, from which we drew 1,000 Monte Carlo realisations per hexagon and year. This captures the heavy-tailed distribution of disturbance activity, allowing extreme but infrequent disturbance pulses to appear in the forecasts (Senf et al., 2025).

Biomass exposure simulation: For each Monte Carlo simulation and year, forecasted disturbed areas were converted to carbon exposure by multiplying them by biomass values sampled from two composition-specific scenarios:

- Early scenario: biomass distribution of forests disturbed during 2011-2016
- Recent scenario: biomass distribution of forests disturbed during 2017-2023

Here, biomass carbon exposure is defined as the amount of aboveground carbon stock affected by disturbance and therefore conditionally vulnerable to future carbon loss under the two disturbance-biomass scenarios. For every hexagon and biomass ensemble member, a biomass value was drawn from the scenario distribution and multiplied by the simulated disturbed area. This produced a time series of biomass exposure per hexagon, year, and disturbance type across 1,000 simulations. Results were aggregated across ensemble members, simulations, and hexagons to compute per-year medians and 5th-95th percentiles at both the hexagon and pan-European scales. This framework links area-based disturbance forecasts with uncertainty in biomass composition, providing scenario-explicit estimates of future carbon exposure.

3 Results

3.1 Shift in disturbance susceptibility toward older, high-biomass forests.

Satellite-based observations revealed an increase in age selectivity since 2017, with natural disturbances disproportionately affecting older and more carbon-dense forests. The area disturbed annually in forests >60 years old nearly tripled between

https://doi.org/10.5194/egusphere-2025-6288
Preprint. Discussion started: 19 December 2025

early (2011-2016) and recent (2017-2023) periods, rising from 0.38 Mha to 1.06 Mha, while disturbances in younger forests increased more modestly from 0.35 to 0.56 Mha (Table S1). This shift is most evident in the joint distribution of forest age and aboveground carbon stocks: recent disturbances increasingly concentrate in stands exceeding both 60 years and 80 MgC ha^{-1} (Fig. 1a,c). The most substantial biomass losses occurred in mature spruce forests in Central and Eastern Europe (Fig. S5a, c).

To quantify the magnitude and spatial pattern of this structural change, we computed the Energy Distance (ED) between the age distributions of disturbed forests in the two periods. ED measures distributional divergence: higher values indicate that recent disturbances affected age classes that differ substantially from those in earlier periods. Natural disturbances showed greater distributional shifts (median ED: 1.5 years; 5th-95th percentile: 1.0-2.3) than harvests (median: 0.9 years; 5th-95th percentile: 0.6-1.3), with peak values in Central and Eastern Europe (Fig. 2a). Critically, this structural change was directional: 64% of grid cells showed increases in the median age of disturbed stands (Fig. 2c), and the concentration of values above the 1:1 line in Fig. 2d confirms that recent disturbances systematically targeted older cohorts.

Regional patterns revealed substantial heterogeneity in this continental trend. In Western and Central Europe, disturbances after 2017 were increasingly concentrated in stands older than 60 years (Fig. S4c,e), consistent with compound drought-amplified bark beetle dynamics in spruce-dominated regions. Northern Europe showed comparatively stable age distributions, with younger stands remaining dominant, though gradual ageing was evident (Fig. S4a). In Eastern and Southeastern Europe, disturbances more frequently affected forests ≤60 years old, particularly 40-50-year-old monospecific pine and spruce plantations, a pattern consistent with high stem densities and drought stress in even-aged stands.

In contrast to natural disturbances, harvest patterns showed structural stability. Harvests remained concentrated in older stands (>60 years) but typically targeted lower-biomass forests than those affected by natural disturbances (Fig. 1b, d; Fig. S3b, d). While harvested area increased substantially (from 4.93 to 6.75 Mha), the age and biomass distributions shifted only modestly (median ED: 0.9 years), with slight increases in mid-aged stands (60-100 years; 40-80 MgC ha^{-1}) likely reflecting salvage operations in beetle-affected regions (Fig. 2b). The contrast between stable harvest selectivity and shifting natural disturbance patterns suggests that climate-amplified biotic agents, rather than management changes, drive the observed structural selectivity.

https://doi.org/10.5194/egusphere-2025-6288
Preprint. Discussion started: 19 December 2025

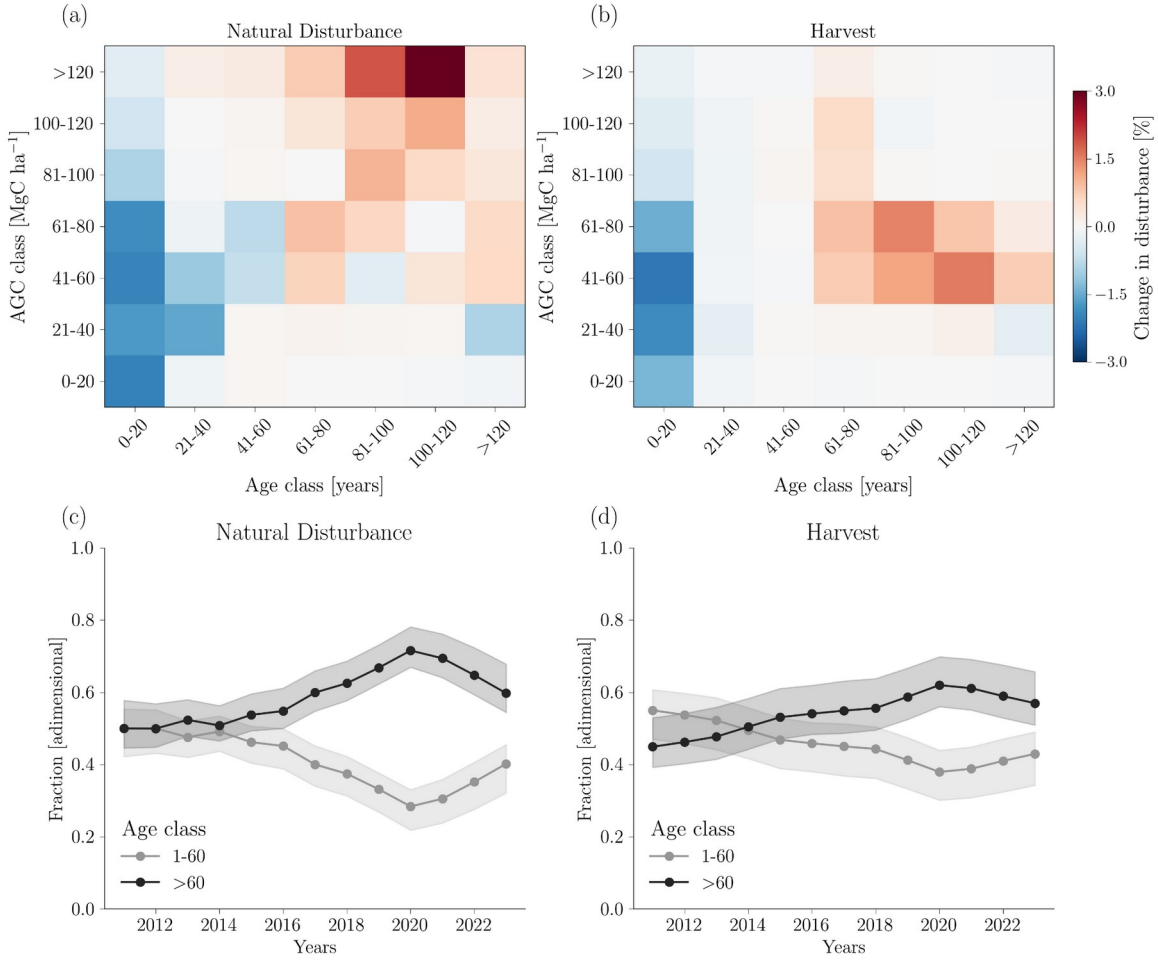

Figure 1: Structural characteristics of forests affected by natural disturbances and harvest across Europe. (a-b) Change in the fraction of disturbed forests between 2017-2023 and 2011-2016 across combinations of aboveground carbon (AGC) class (Mg C ha^{-1}) and forest age class (years). Warmer colours (reds) indicate increased disturbance in that class; cooler colours (blues) indicate a decline. (c-d) Temporal evolution of the fraction of disturbed area by forest age class (1-60 years vs. >60 years) for natural disturbances (c) and harvest (d) from 2011 to 2023. Shaded ribbons represent the 95% quantile range across the 20-member forest age ensemble, and lines show the median trajectory. Only 100 m pixels with at least 30% forest cover were retained, and among those, only pixels where at least 50% of the forested area was disturbed by a specific agent in a given year were considered.

https://doi.org/10.5194/egusphere-2025-6288
Preprint. Discussion started: 19 December 2025

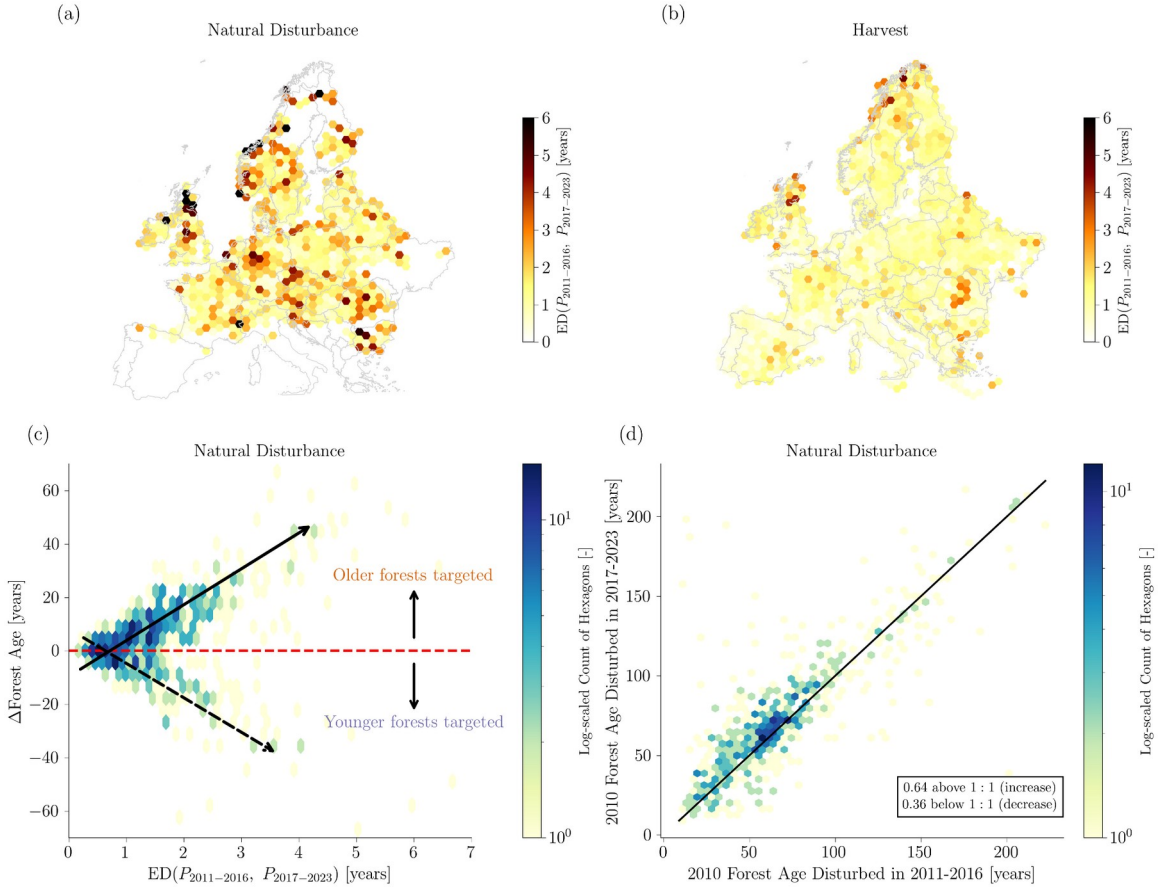

Figure 2: Structural changes in disturbed forest stands over time, quantified with the energy distance metric. (a-b) Spatial distribution of energy distance values comparing forest age distributions affected by natural disturbances (a) and harvest (b) between two periods (2011-2016 vs. 2017-2023). Higher values indicate greater temporal dissimilarity in the age of disturbed forests. (c) Relationship between ED and the direction of structural change (ΔForest Age). Because all ages are fixed to 2010 values, the differences reflect selection, not regrowth or mortality. Positive Δ values indicate a shift toward forest disturbance, specifically a growing tendency to affect older stands in later periods, independent of natural forest ageing. (d) Comparison of the 2010 baseline forest age for disturbances occurring in 2011-2016 (x-axis) and 2017-2023 (y-axis). Values above the 1:1 line indicate that forests disturbed in the later period were generally older than those disturbed earlier, while values below the line reflect a shift toward younger stands. Only 100 m pixels with at least 30% forest cover were retained, and among those, only pixels where at least 50% of the forested area was disturbed by a specific agent in a given year were considered. Hexagons with fewer than 50 valid pixels per period were excluded from analysis. Each hexagon has a diameter of approximately 100 km. Hexagons were used as aggregation units because they offer equal-distance neighbour relationships and minimise edge effects compared to squares.

https://doi.org/10.5194/egusphere-2025-6288
Preprint. Discussion started: 19 December 2025

3.2 High-biomass spruce stands are disproportionately affected by natural disturbances.

Spruce-dominated forests exhibited the strongest structural shift in disturbance impacts, with natural disturbances increasingly concentrated in high-biomass stands during the period 2017-2023 (Fig. 3; Fig. S5). Biomass carbon losses from natural disturbances in spruce forests increased nearly eightfold between periods, from 5.9 TgC (5th-95th percentile: 4.9-7.2) in 2011-2016 to 45.4 TgC (37.9-54.2) in 2017-2023. This increase outpaced the sixfold expansion in disturbed area (from 0.07 to 0.46 Mha; Table S2), indicating a disproportionate rise in carbon losses relative to disturbance extent.

This disproportionate increase reflects a systematic shift toward higher-biomass cohorts. Median biomass of disturbed spruce stands rose from approximately 75 to 95 MgC ha^{-1} between periods (Cohen's d = 1.0, indicating a large effect; Fig. 3a,c), demonstrating that recent disturbances increasingly affected structurally mature spruce forests. The spatial concentration of this shift in Central Europe (Fig. S5a), where high-biomass spruce monocultures are prevalent, further highlights the role of forest structure in amplifying disturbance-related carbon impacts.

Together, expanding disturbance extent and increasing per-hectare biomass resulted in a disproportionate increase in carbon losses from spruce forests. Although spruce accounted for only ~30 % of the total naturally disturbed area in the recent period, it contributed approximately 40 % of natural-disturbance-related biomass carbon losses. This contrasts sharply with other forest types. In other coniferous and broadleaf forests, biomass losses from natural disturbances increased more gradually, from 16.7 to 37.9 TgC (+127 %) and from 20.5 to 32.2 TgC (+57 %), respectively (Fig. 3c). These increases closely tracked expansions in disturbed area (0.26 to 0.53 Mha in other conifers; 0.30 to 0.46 Mha in broadleaves) and were not accompanied by significant shifts in the biomass structure of affected stands (median biomass stable; effect sizes < 0.5; Fig. 3a).

Harvest-related biomass losses also increased across all forest types (Fig. 3d), but in contrast to natural disturbances, these trends were driven almost entirely by expanding harvested area rather than by structural selectivity. Harvested area expanded from 0.28 to 0.90 Mha in spruce, from 1.85 to 2.8 Mha in other conifers, and from 2.2 to 2.4 Mha in broadleaf forests, while the biomass distribution of harvested stands remained stable (Fig. 3b). Consequently, most harvest-related biomass losses originated from broadleaf (115.8 and 123.6 TgC in 2011-2016 and 2017-2023, respectively) and other coniferous forests (96.7 and 148.6 TgC), with spruce contributing a smaller but increasing share (18.8 and 59.0 TgC). This contrast underscores that the disproportionate increase in carbon losses observed in spruce forests arises primarily from climate-driven natural disturbances interacting with forest structure, rather than from shifts in management practices.

https://doi.org/10.5194/egusphere-2025-6288
Preprint. Discussion started: 19 December 2025

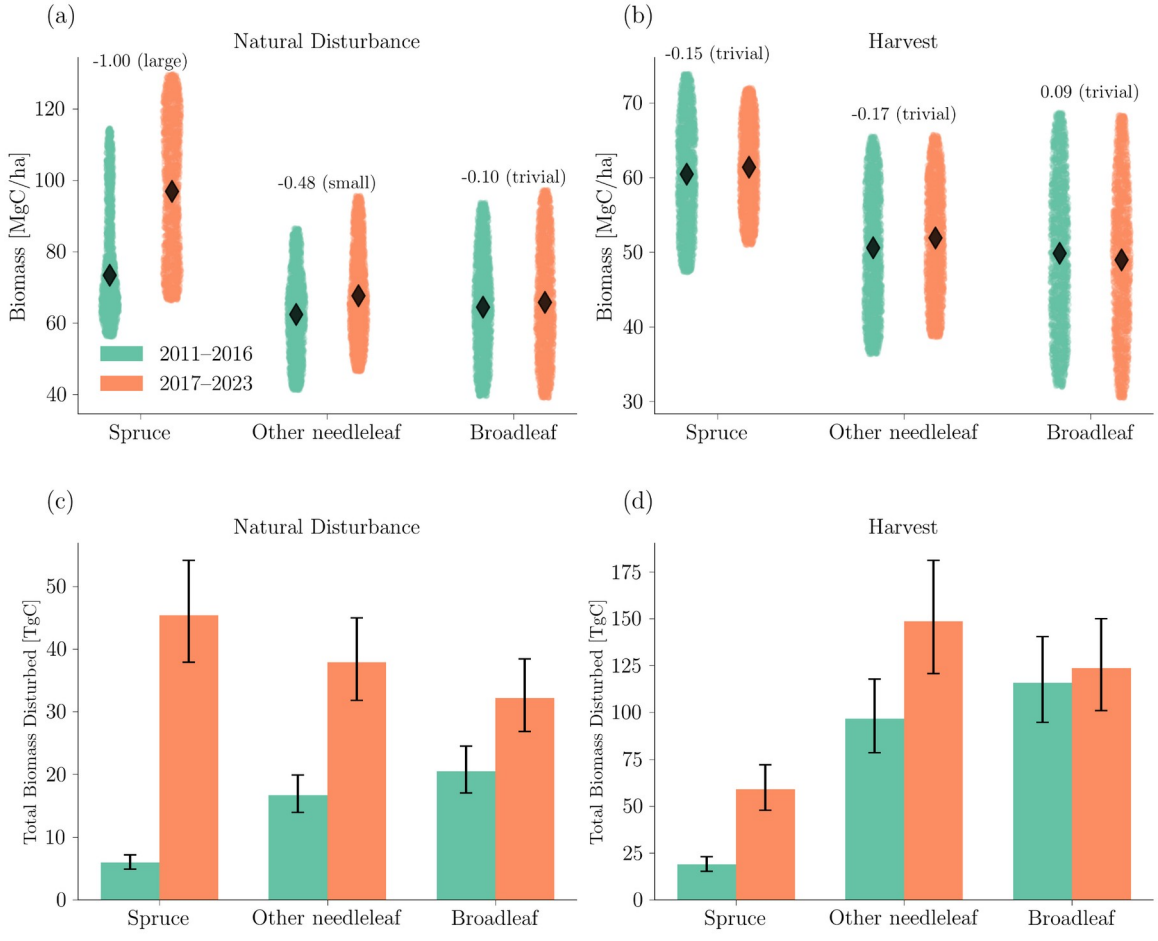

Figure 3: Structural and quantitative changes in aboveground carbon loss by species group for natural forest disturbances and harvests. (a-b) Median biomass of disturbed forest stands by dominant tree genus for natural disturbances (a) and harvest (b), comparing early (2011-2016) and recent (2017-2023) periods. Each point in the jitter plots represents a pixel. Annotated values represent Cohen's d effect sizes, quantifying the standardised difference in median biomass between periods for each species group. (c-d) Total AGB loss (TgC) by species group from natural disturbances (c) and harvest (d) in both periods. Bars indicate the median across a 20-member biomass ensemble, and error bars represent the 5th and 95th percentiles, capturing uncertainty in biomass estimates. Only 100 m pixels with at least 30% forest cover were retained, and among those, only pixels where at least 50% of the forested area was disturbed by a specific agent in a given year were considered.

https://doi.org/10.5194/egusphere-2025-6288
Preprint. Discussion started: 19 December 2025

3.3 Natural disturbances increasingly occur in structurally homogeneous forests.

Beyond targeting older, high-biomass forests, natural disturbances are increasingly concentrated in structurally homogeneous stands. Between 2011-2016 and 2017-2023, natural disturbances shifted markedly toward such stands, as indicated by declining coefficients of variation (CV) in pre-disturbance biomass, particularly in Central and Eastern Europe (Fig. 4a). By contrast, harvest-related CV changes were spatially diffuse and lacked the geographic clustering characteristic of climate-driven bark beetle outbreaks (Fig. 4b).

This shift toward homogeneous stands was strongly genus-specific (Fig. 4c). Spruce-dominated stands exhibited a pronounced decline in CV (Cohen's d = 1.25), indicating that recent disturbances targeted structurally uniform spruce forests. This effect size is large, larger even than the shift toward high-biomass stands (Section 3.2; d = 1.0), and suggests that structural homogeneity may be as crucial as stand age in determining bark beetle susceptibility. By contrast, broadleaf (Cohen's d = 0.22) and other needleleaf forests (Cohen's d = 0.55) showed weak to moderate declines, confirming that the homogeneity signal is driven by spruce monocultures in Central Europe.

The shift toward structurally homogeneous stands was not only a snapshot difference between periods but an ongoing temporal trend. In spruce forests, the CV of pre-disturbance biomass declined significantly over time in both naturally disturbed (slope = -0.0043 yr^{-1}, p = 0.002) and harvested (slope = -0.0043 yr^{-1}, p = 0.003) stands, equivalent to a ~6% reduction in CV over the 2011-2023 period (Fig. 4d). Remarkably, natural disturbances and harvests showed nearly identical downward trajectories (Pearson's r = 0.75), suggesting both agents increasingly target the same structurally uniform stands, likely reflecting salvage operations following bark beetle infestations. By contrast, broadleaf and other needleleaf forests showed no significant temporal trends in CV (Fig. S6b,c), and the strong spruce signal dominated the continental-scale average. Across all genera, harvested stands consistently exhibited higher CV than naturally disturbed stands (Pearson's r = 0.90), consistent with the interpretation that natural disturbances disproportionately affect the most homogeneous forests.

https://doi.org/10.5194/egusphere-2025-6288
Preprint. Discussion started: 19 December 2025

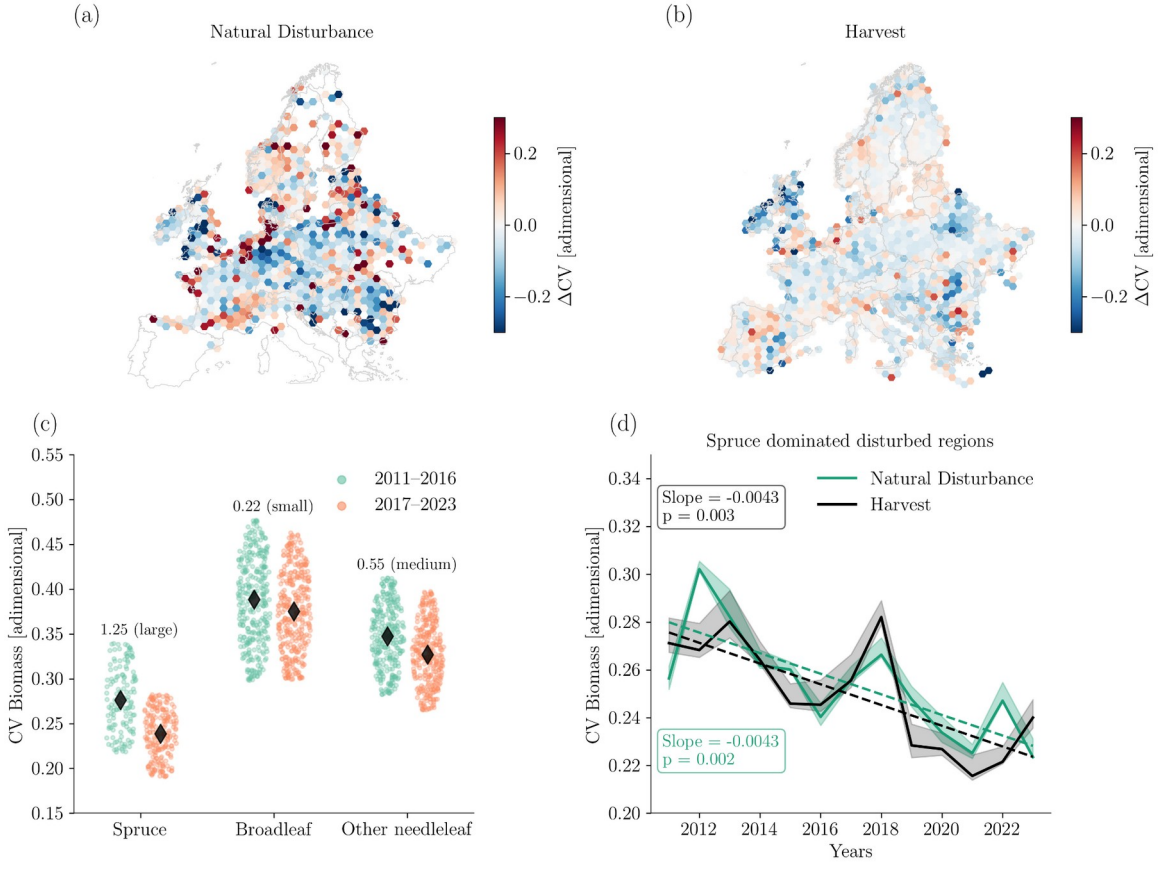

Figure 4: Changes in structural heterogeneity of disturbed forests across Europe. (a, b) Spatial changes in the coefficient of variation (CV) of aboveground biomass within disturbed pixels between 2011-2016 and 2017-2023, shown for (a) natural disturbances and (b) harvest. Blue shades indicate declining CV (more homogeneous stands), and red shades indicate increasing CV (more heterogeneous stands). (c) CV of biomass in disturbed pixels by genus group (spruce, broadleaf, other needleleaf) and period. Cohen's *d* effect sizes are reported above each comparison. (d) Temporal evolution of biomass CV in disturbed spruce-dominated pixels from 2011 to 2023, shown separately for natural disturbances and harvest. Lines represent the annual median CV across hexagons; shaded ribbons indicate the 5th to 95th percentile range across biomass members. Only 100 m pixels with at least 30% forest cover were retained, and among those, only pixels where at least 50% of the forested area was disturbed by a specific agent in a given year were considered. Each hexagon has a diameter of 100 km.

https://doi.org/10.5194/egusphere-2025-6288
Preprint. Discussion started: 19 December 2025

3.4 Amplifying biomass carbon exposure from natural disturbances.

If current disturbance patterns persist, natural disturbances alone could expose biomass carbon equivalent to approximately 20% of Europe's contemporary forest carbon sink (~210 TgC yr^{-1}) (Pan et al., 2024) by 2040. Under the recent biomass scenario, projected exposure reaches a median of ~46 TgC yr^{-1} (Fig. 5c), indicating that the carbon consequences of disturbance are intensifying beyond what would be expected from expanding disturbance area alone. This exposure represents carbon stocks transferred out of live forest biomass pools and rendered vulnerable to delayed recovery or longer-term loss, rather than immediate atmospheric fluxes. The projected exposure is geographically concentrated: Central European spruce forests, particularly the Bohemian Massif and surrounding mid-elevation ranges, emerge as primary hotspots under both scenarios (Fig. 5a). In contrast, harvest-related biomass carbon exposure, while larger in absolute magnitude (~134 TgC yr^{-1}), remains structurally stable and is concentrated mainly in Northern Europe (Fig. 5b).

Structural shifts toward older, higher-biomass, and more homogeneous stands substantially amplify future carbon exposure. Comparing the two scenarios isolates this effect: the early scenario uses the 2011-2016 biomass distribution of disturbed stands to forecast disturbance areas, whereas the recent scenario uses the 2017-2023 distribution. Under the recent scenario, natural disturbances are projected to expose a median of 46.3 TgC yr^{-1} (5th-95th percentile: 38.3-56.4), compared to 41.9 TgC yr^{-1} (34.4-51.2) under the early scenario, an increase of 10.5% attributable primarily to the growing involvement of carbon-rich cohorts. Over the 2024-2040 projection period, this structural shift compounds to an additional ~75 TgC of biomass carbon exposure, equivalent to roughly one-third of Europe's annual forest carbon sink. By contrast, projected harvest-related biomass exposure remains structurally stable across scenarios (131.0 vs. 133.6 TgC yr^{-1}; <2% change), indicating that harvest practices have not shifted toward systematically higher-biomass stands, as observed for natural disturbances.

This projected increasing carbon exposure results from the combined effects of expanding disturbance extent and increasing per-hectare biomass affected. Natural disturbances are projected to nearly double in spatial extent, from 0.36 Mha (0.19-0.70 Mha) in 2024 to 0.58 Mha (0.31-0.99 Mha) by 2040, whereas harvest expansion is more gradual (1.93 to 2.38 Mha; Fig. 5d). The steeper trajectory for natural disturbances reflects climate-driven amplification of bark beetle dynamics, while harvest areas remain aligned with management objectives and policy constraints. This interaction creates a multiplicative risk: even if future disturbance extent stabilises, continued targeting of carbon-rich forests would sustain elevated levels of biomass carbon exposure, thereby weakening the long-term effectiveness of Europe's forest carbon sink.

https://doi.org/10.5194/egusphere-2025-6288
Preprint. Discussion started: 19 December 2025

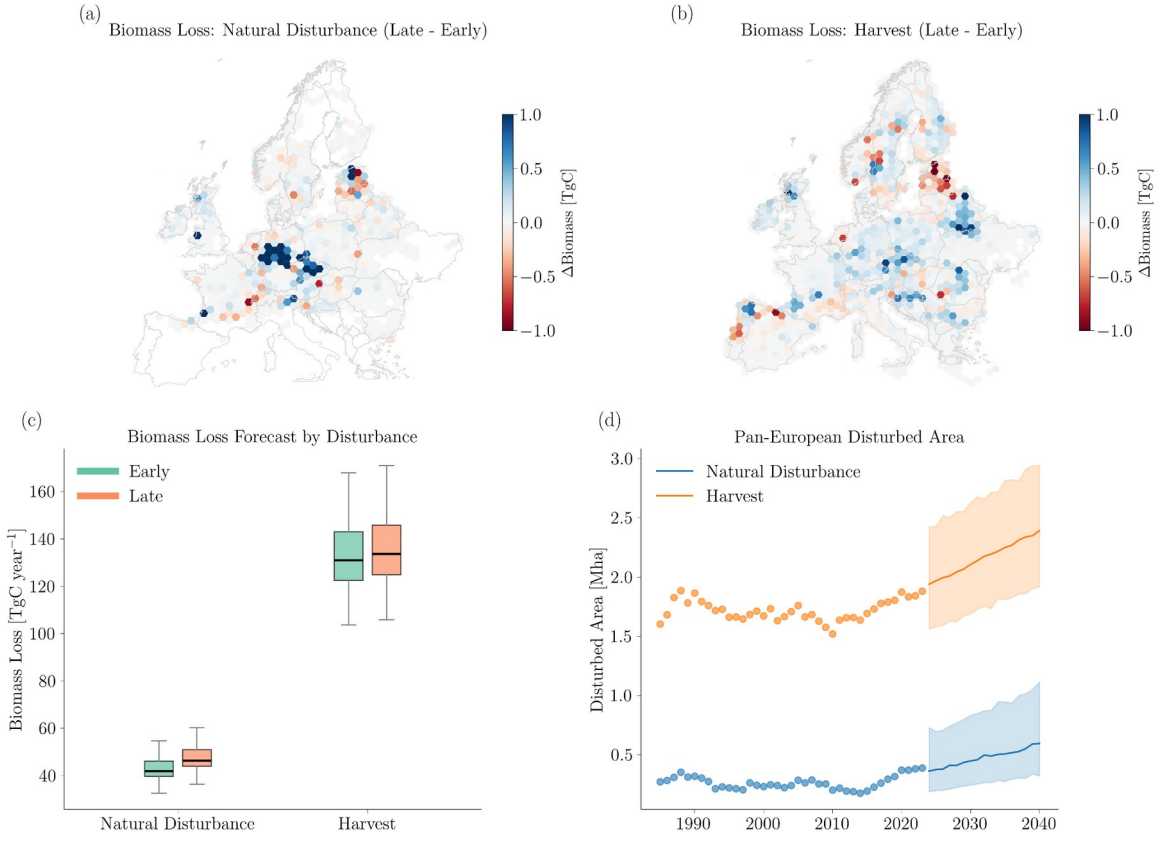

Figure 5: Forecasted biomass exposure and disturbed area across Europe through 2040 under early (2011-2016) and recent (2017-2023) disturbance scenarios. (a-b) Spatial differences in biomass exposure (PgC) between early and recent periods for natural disturbances (a) and harvest (b), with darker colours indicating larger increases in carbon exposure. (c) Boxplots of annual biomass exposure (TgC yr^{-1}) by disturbance type and scenario. Forecasts are based on smoothed trends (1985-2023), and model fits to the 2008-2023 window, assuming no change in forest management or spatial disturbance extent. Boxes represent the median and interquartile range across 20 biomass ensemble members; whiskers show the 5th and 95th percentiles. (d) Forecasted area of pan-European disturbed forests annually by natural disturbances and harvest. Points represent observed values (1985-2023); solid lines and shaded bands represent trend-based projections and their uncertainty ranges. Only 100 m pixels with at least 30% forest cover were retained, and among those, only pixels where at least 50% of the forested area was disturbed by a specific agent in a given year were considered. Hexagons with fewer than 50 valid pixels were excluded from analysis. Each hexagon has a diameter of 100 km.

Genus-specific projections show that spruce forests drive the amplification of biomass carbon exposure associated with natural disturbances (Fig. 6a). Under the recent scenario, spruce-dominated forests are projected to experience a median biomass carbon exposure of 18.5 TgC yr^{-1} (5th-95th percentile: 17.3-20.2), representing a 16% increase relative to the early

https://doi.org/10.5194/egusphere-2025-6288
Preprint. Discussion started: 19 December 2025

scenario (16.0 TgC yr⁻¹). In contrast, other needleleaf and broadleaf forests show only minor differences between scenarios (9.0 vs. 8.6 TgC yr^{-1} and 17.9 vs. 16.6 TgC yr^{-1}, respectively), indicating that their disturbance-related carbon exposure scales primarily with expanding affected area rather than with shifts toward higher-biomass structural cohorts.

Harvest-related projections exhibit comparatively stable patterns across scenarios, with biomass carbon exposure dominated by broadleaf (47.4-47.7 TgC yr⁻¹) and other needleleaf forests (65.7-66.4 TgC yr⁻¹; Fig. 6b). Exposure associated with spruce harvests increases modestly (from 10.3 to 11.2 TgC yr⁻¹), likely reflecting enhanced salvage activity in beetle-affected regions rather than systematic shifts in planned harvest toward higher-biomass stands.

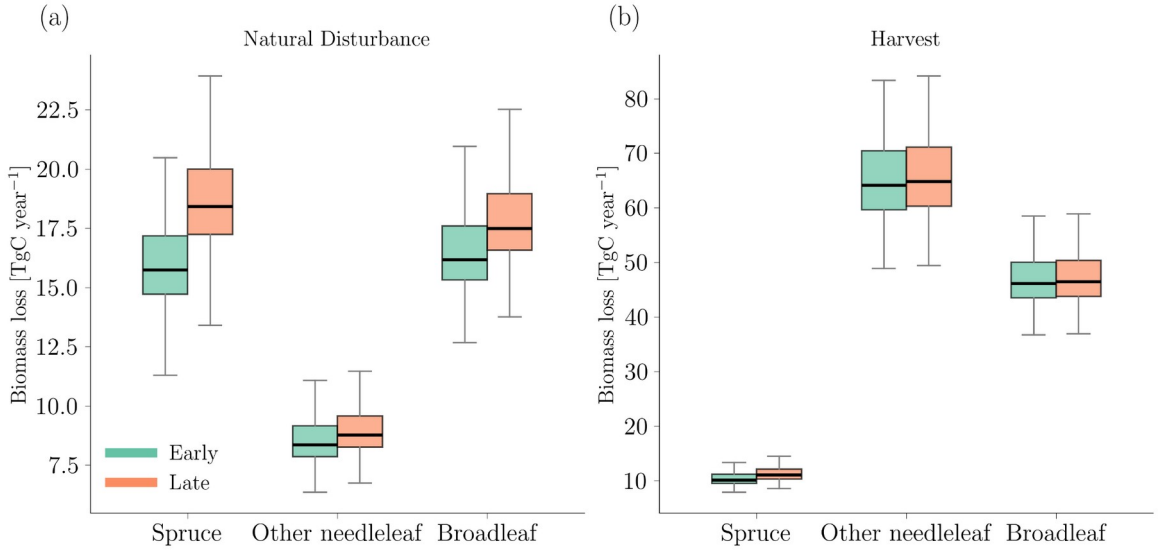

Figure 6: Forecasted biomass exposure across Europe through 2040 under early (2011-2016) and recent (2017-2023) disturbance scenarios and across dominant species. (a-b) Boxplots of annual biomass exposure (TgC yr^{-1}) for natural disturbances and harvest, stratified by scenario (early vs. recent) and by the dominant species group of each hexagon. The dominant species was assigned as the genus class occupying the largest forested area within each 100-km hexagon. Forecasts are based on smoothed trends (1985-2023), and model fits to the 2008-2023 window, assuming no change in forest management or spatial disturbance extent. Boxes represent the median and interquartile range across 20 biomass ensemble members; whiskers show the 5th and 95th percentiles. Only 100 m pixels with at least 30% forest cover were retained, and among those, only pixels where at least 50% of the forested area was disturbed by a specific agent in a given year were considered. Hexagons with fewer than 50 valid pixels were excluded from analysis.

https://doi.org/10.5194/egusphere-2025-6288
Preprint. Discussion started: 19 December 2025

4 Discussion

Europe's forests face a compound vulnerability: climate-driven disturbances are increasingly concentrated in the continent's oldest, most carbon-dense stands, precisely those that underpin long-term carbon storage and took decades to develop. Our continental-scale analysis reveals that this structural selectivity occurs along three interacting dimensions: stand age, aboveground biomass, and structural homogeneity. Natural disturbances in forests >60 years old nearly tripled between 2011-2016 and 2017-2023 (0.38 to 1.08 Mha), with impacts increasingly concentrated in stands exceeding 80 MgC ha^{-1} and exhibiting low biomass variation (CV decline: Cohen's d = 1.25 in spruce). This pattern represents not only an expansion of the extent of disturbance but also a qualitative shift in the forest structures most frequently affected, and therefore in the carbon stocks most exposed to rapid transfer from live-biomass pools. If these patterns persist, natural disturbances could expose biomass carbon equivalent to approximately 20% of Europe's contemporary forest carbon sink (~46 of ~210 TgC yr^{-1}) by 2040, with risks concentrated primarily in Central European spruce-dominated landscapes.

The observed shift in disturbance selectivity aligns spatially and temporally with climate-amplified bark beetle dynamics in spruce-dominated regions. Compound drought and heat events since 2018 have predisposed mature spruce stands to infestation, creating conditions for unprecedented intensification of outbreaks (Hermann et al., 2023; Weynants et al., 2024). Warming accelerates beetle development, enabling multiple generations per year and facilitating expansion into higher elevations and latitudes where historically cold temperatures had constrained outbreaks (Hartmann et al., 2025; Jakoby et al., 2019). While windstorms have historically caused episodic, large-scale forest losses (e.g., Lothar 1999, Klaus 2009), their spatially localised and temporally discrete nature does not align with the broad spatial coherence and multi-year persistence of the structural shift observed since 2017, a period during which bark beetles dominated disturbance activity across much of Central Europe (Patacca et al., 2023).

Structural homogeneity is associated with heightened susceptibility. Even-aged spruce monocultures provide continuous host connectivity, facilitating rapid beetle spread once outbreaks are initiated (Raffa et al., 2008). Such stands also lack vertical and horizontal structural complexity, reducing microclimatic buffering and increasing exposure to drought stress and heat accumulation, which further weakens host resistance (Senf and Seidl, 2018). Heterogeneous forests, by contrast, fragment host networks, maintain cooler and moister microclimates, and provide refugia for beetle predators and competitors (Seidl et al., 2016).

Large-scale natural disturbances in Europe are frequently followed by salvage logging, which often leads to the re-establishment of extensive, even-aged spruce stands on affected sites (Sommerfeld et al., 2021). These post-disturbance management responses may contribute to maintaining, rather than disrupting, the structural conditions associated with high susceptibility, limiting the development of structural complexity that could otherwise enhance resistance. The near-identical temporal trajectories of CV decline in both naturally disturbed and harvested spruce stands (Pearson's r = 0.75) indicate a

https://doi.org/10.5194/egusphere-2025-6288
Preprint. Discussion started: 19 December 2025

strong coupling between disturbance processes and management responses, suggesting that harvest activity increasingly mirrors disturbance patterns rather than proactively reducing long-term vulnerability. This coupling is most pronounced in Central Europe, where decades of homogeneous spruce planting have produced landscapes highly prone to outbreak amplification under climate stress.

Outbreak dynamics further reinforce this structural vulnerability. Early in disturbance cycles, infestations often target physiologically weakened hosts; however, during outbreak peaks, such as those following the 2018 drought, high beetle populations can overwhelm even relatively vigorous trees, diminishing the role of individual tree resistance and further concentrating impacts in structurally uniform landscapes (Senf and Seidl, 2021). Together with the homogenising effects of salvage logging, these dynamics help explain why spruce-dominated regions exhibit the most substantial and most persistent declines in structural heterogeneity, and why homogeneous stands continue to incur disproportionate disturbance impacts even as climate stress expands susceptibility to younger pine and spruce plantations in parts of Eastern Europe (Davydenko et al., 2021; Siitonen, 2014).

The three dimensions of structural selectivity we document (i.e, age, biomass, and homogeneity) are closely linked rather than independent. Older stands tend to accumulate higher biomass over decades of growth, and Central European spruce monocultures frequently combine advanced age (>60 years), high carbon density (>80 MgC ha^{-1}), and low structural diversity. Our results indicate that forests combining these characteristics exhibit disproportionately high exposure. Such stands dominate the Bohemian Massif and surrounding mid-elevation ranges of Austria, Germany, and the Czech Republic, consistent with the geographic concentration of disturbance-related carbon exposure identified in our spatial projections (Fig. 5a).

This convergence of vulnerabilities explains why a relatively small fraction of Europe's forest area contributes disproportionately to disturbance-related carbon exposure. Spruce forests accounted for roughly 30% of the naturally disturbed area in the recent period, yet contributed approximately 40% of disturbance-associated biomass carbon losses, with an eight-fold increase between periods (5.9 to 45.4 TgC). Regional contrasts further support this interpretation: Western and Central Europe experienced pronounced shifts toward older impacted cohorts beginning around 2017, coinciding with prolonged compound drought conditions through 2022. In contrast, parts of Eastern and Southeastern Europe showed relatively greater impacts in younger (approximately 40-50 years old) pine and spruce plantations, which often exhibit high stem densities, limited thinning, and elevated drought sensitivity (Jaime et al., 2022).

The compound nature of this vulnerability implies that effective climate adaptation cannot rely on single-axis interventions. Age diversification alone may not protect structurally homogeneous spruce stands from drought-amplified beetle outbreaks; species diversification without increased structural complexity may merely shift the vulnerable cohort; and structural

https://doi.org/10.5194/egusphere-2025-6288
Preprint. Discussion started: 19 December 2025

thinning in climatically marginal regions may, in some cases, exacerbate drought stress. Reducing future susceptibility will likely require coordinated management of species composition, structural complexity, and spatial heterogeneity.

Our projection that natural disturbances could expose biomass carbon equivalent to approximately 20% of Europe's forest carbon sink by 2040 is conservative by design. We assume no further geographic expansion of bark beetle outbreaks beyond current ranges, despite documented upward and northward spread (Hartmann et al., 2025, Junttila et al., 2024; Kärvemo et al., 2023). We also exclude post-disturbance mortality cascades and assume historical recovery rates, even though recurrent disturbances increasingly slow regrowth and may induce persistent ecosystem state shifts (Forzieri et al., 2022; Senf and Seidl, 2022). Management practices are held constant, although future changes in harvesting, salvage strategies, or species composition could substantially alter disturbance exposure.

Each of these excluded processes would tend to amplify, rather than dampen, projected carbon exposure. Forecast uncertainty remains substantial, with 5th-95th percentile ranges spanning approximately ±20% around median estimates (Fig. 5c), reflecting interannual variability in disturbance activity (captured via Taylor's law variance scaling; Taylor, 1961), uncertainty in biomass estimates, and stochastic extremes such as storm events or outbreak collapses (Senf et al., 2025). Notably, even the lower bounds of projected natural-disturbance-related biomass exposure (34-38 TgC yr^{-1}) exceed upper estimates from the early 2010s (~7 TgC yr^{-1}; Section 3.2), indicating that intensification is robust across plausible trajectories. Accordingly, the estimated 20% sink offset should be interpreted as a near-term baseline risk rather than a worst-case outcome.

5 Conclusion

Our findings reveal a clear divergence in contemporary disturbance dynamics across Europe's forests. Natural disturbances increasingly affect older, carbon-dense spruce stands in Northern and Central Europe. In contrast, harvest activities remain structurally stable and are more frequently concentrated in younger or lower-biomass forests. This divergence reflects a growing structural selectivity of climate-sensitive natural disturbances, particularly bark beetle outbreaks, which now disproportionately expose carbon-rich and structurally mature forest cohorts. As a result, disturbance impacts are not only expanding in area but are increasingly concentrated in forest structures that store large amounts of biomass accumulated over decades.

The concentration of disturbance impacts in these vulnerable cohorts implies that Europe's disturbance-related carbon exposure is likely to intensify and spatially consolidate in regions dominated by mature spruce forests. Because recovery rates in older, high-biomass stands are typically slower and marginal carbon uptake is lower than in younger forests, disturbances affecting these cohorts have disproportionate implications for long-term forest carbon storage, even when

https://doi.org/10.5194/egusphere-2025-6288
Preprint. Discussion started: 19 December 2025

regrowth ultimately occurs. Consequently, moderate increases in disturbance frequency or extent can translate into amplified, continent-scale reductions in the effectiveness of the forest carbon sink.

If current trajectories persist, natural disturbances alone could expose a substantial share of Europe's land-based forest carbon sequestration capacity over the coming decades. Addressing this emerging risk requires re-evaluating the drivers of forest structural vulnerability and implementing adaptive management strategies that enhance resilience to climate-sensitive disturbances. Proposed measures include increasing species and structural diversity, reducing susceptibility in high-risk stands, and refining harvest and post-disturbance management practices in disturbance-prone regions (Migliavacca et al., 2025). The effectiveness of such strategies will depend on their ability to reduce structural homogeneity and interrupt feedback between disturbance processes and management responses.

Improved monitoring of disturbance and mortality remains crucial for predicting carbon losses and informing policy. This includes coordinated, EU-wide data collection (Network, 2025; Zweifel et al., 2023) and collaborative platforms, such as *deadtrees.earth* (Mosig et al., 2024). Integrating national assessments into open-access systems would strengthen both scientific modelling and policy implementation under frameworks such as the EU Forest Strategy for 2030 ("Communication," n.d.), the LULUCF Regulation (Regulation (EU) 2023/839) ("Regulation - 2023/839 - EN - EUR-Lex," n.d.), and the Nature Restoration Regulation (Regulation (EU) 2024/1991) ("Regulation - EU - 2024/1991 - EN - EUR-Lex," n.d.). As Europe advances these ambitious forest policies, explicitly recognising and mitigating the growing vulnerability of its oldest and most carbon-rich forests will be critical for safeguarding the continent's land carbon sink in a warming climate.

Data availability.

- The European Forest Disturbance Atlas v2.1.1 is available from Viana-Soto and Senf (2025) at https://doi.org/10.5194/essd-17-2373-2025.
- Forest age data (Global Age Mapping Integration v3.0) are available from Besnard et al. (2023) at https://doi.org/10.5880/GFZ.1.4.2023.006.
- Aboveground biomass data (ESA CCI Biomass v6.0) are available from Santoro and Cartus (2023) at https://doi.org/10.5285/AF60720C1E404A9E9D2C145D2B2EAD4E.
- European forest genus classification data are available from De Keersmaecker et al. (2024) at https://doi.org/10.5281/zenodo.13341104.

All processed datasets underlying the analyses and figures presented in this study are publicly available via Zenodo at: **https://doi.org/10.5281/zenodo.17977435**. The Zenodo repository contains aggregated disturbance metrics, forest age and biomass distributions, structural heterogeneity metrics, and projection outputs used to generate the figures. All files are provided in open formats.

https://doi.org/10.5194/egusphere-2025-6288
Preprint. Discussion started: 19 December 2025

Code availability.

All code for data integration, statistical analysis, forecasting, and visualisation is available at https://github.com/simonbesnard1/structshift. The repository includes Python scripts for disturbance-demographic integration, Energy Distance calculations, ensemble forecasting, and figure generation. Documentation and example workflows are provided in the repository README.

Authors contributions

SB designed the research, performed the analysis, and drafted the manuscript. The study builds on an original idea developed by CS. SB also prepared the GAMIv3.0 dataset. AVS and CS prepared the European Forest Disturbance Atlas maps; WDK and RVDK provided the genus distribution maps; and MS prepared the ESA-CCI biomass product. All authors contributed to the interpretation of results and provided critical feedback on the manuscript. This work is the outcome of a research exchange of SB and VH to TU München.

Competing interests.

The authors declare that they have no conflict of interest.

Acknowledgements

We thank the Global Land Monitoring group members at the GFZ Helmholtz Centre for Geosciences for providing feedback on the presented results. We thank the GFZ Helmholtz Centre for Geosciences for providing the computational and data infrastructure that enabled this research. We recognise the use of OpenAI's ChatGPT and Grammarly AI tools to assist with improving sentence structure, clarity, and grammar during manuscript preparation. Importantly, we emphasise that all research design, data analysis, interpretation of results, and conclusions presented in this study are entirely our own.

Financial support

SB and VH acknowledge funding support by the European Union through the FORWARDS (https://forwards-project.eu/), OpenEarthMonitor (https://earthmonitor.org/), and NextGenCarbon (https://www.nextgencarbon-project.eu/) projects. AVS, CS, WDK, and RVDK acknowledge funding from the ForestPaths project (https://forestpaths.eu/). AVS and CS further acknowledge funding from the European Space Agency (CLIMATE SPACE RECCAP2; 4000144908/24/I-LR) and the Federal Ministry of Education and Research (BMBF) (AI4Forest; 01IS23025C).

References

Bergkvist, J., Lagergren, F., Islam, Md.R., Wårlind, D., Miller, P.A., Finnander Linderson, M.-L., Lindeskog, M., Jönsson, A.M., 2025. Quantifying the Impact of Climate Change and Forest Management on Swedish Forest Ecosystems Using the Dynamic Vegetation Model LPJ-GUESS. Earth's Future 13, e2024EF004662. https://doi.org/10.1029/2024EF004662

https://doi.org/10.5194/egusphere-2025-6288
Preprint. Discussion started: 19 December 2025

Besnard, S., Heinrich, V.H.A., Carvalhais, N., Ciais, P., Herold, M., Luijkx, I., Peters, W., Requena Suarez, D., Santoro, M., Yang, H., 2025. Global covariation of forest age transitions with the net carbon balance. Nat. Ecol. Evol. 1–13. https://doi.org/10.1038/s41559-025-02821-5

Besnard, S., Koirala, S., Santoro, M., Weber, U., Nelson, J., Gütter, J., Herault, B., Kassi, J., N'Guessan, A., Neigh, C., Poulter, B., Zhang, T., Carvalhais, N., 2021. Mapping global forest age from forest inventories, biomass and climate data. Earth Syst. Sci. Data 13, 4881–4896. https://doi.org/10.5194/essd-13-4881-2021

Besnard, S., Santoro, M., Herold, M., Cartus, Oliver, Gütter, J., Heinrich, V.H.A., Herault, B., Kassi, J., Koirala, S., N'Guessan, A., Neigh, C., Nelson, J.A., Poulter, B., Weber, U., Zhang, T., Carvalhais, N., n.d. Global Age Mapping Integration (GAMI). V. 2.0. https://doi.org/10.5880/GFZ.1.4.2023.006

Brockerhoff, E.G., Jactel, H., Parrotta, J.A., Quine, C.P., Sayer, J., 2008. Plantation forests and biodiversity: oxymoron or opportunity? Biodivers. Conserv. 17, 925–951. https://doi.org/10.1007/s10531-008-9380-x

Calle, L., Poulter, B., 2021. Ecosystem age-class dynamics and distribution in the LPJ-wsl v2.0 global ecosystem model. Geosci. Model Dev. 14, 2575–2601. https://doi.org/10.5194/gmd-14-2575-2021

Ceccherini, G., Duveiller, G., Grassi, G., Lemoine, G., Avitabile, V., Pilli, R., Cescatti, A., 2020. Abrupt increase in harvested forest area over Europe after 2015. Nature 583, 72–77. https://doi.org/10.1038/s41586-020-2438-y

Communication: New EU Forest Strategy for 2030 | European Commission [WWW Document], n.d. URL https://commission.europa.eu/document/cf3294e1-8358-4c93-8de4-3e1503b95201_en (accessed 7.30.25).

Davydenko, K., Vasaitis, R., Elfstrand, M., Baturkin, D., Meshkova, V., Menkis, A., 2021. Fungal Communities Vectored by Ips sexdentatus in Declining Pinus sylvestris in Ukraine: Focus on Occurrence and Pathogenicity of Ophiostomatoid Species. Insects 12, 1119. https://doi.org/10.3390/insects12121119

De Keersmaecker, W., Zanaga, D., Viana-Soto, A., Senf, C., Van De Kerchove, R., 2024. ForestPaths: European genus map.

Forzieri, G., Dakos, V., McDowell, N.G., Ramdane, A., Cescatti, A., 2022. Emerging signals of declining forest resilience under climate change. Nature 608, 534–539. https://doi.org/10.1038/s41586-022-04959-9

Hansen, M.C., Potapov, P.V., Moore, R., Hancher, M., Turubanova, S.A., Tyukavina, A., Thau, D., Stehman, S.V., Goetz, S.J., Loveland, T.R., Kommareddy, A., Egorov, A., Chini, L., Justice, C.O., Townshend, J.R.G., 2013. High-Resolution Global Maps of 21st-Century Forest Cover Change. Science 342, 850–853. https://doi.org/10.1126/science.1244693

Hartmann, H., Battisti, A., Brockerhoff, E., Bełka, M., Hurling, R., Jactel, H., Oliva, J., Rousselet, J., Terhonen, E., Ylioja, T., Melin, M., Olson, Å., De Prins, F., Zhang, K., Stein Åslund, M., Davydenko, K., Menkis, A., Elfstrand, M., Zúbrik, M., Kunca, A., Galko, J., Paulin, M., Csóka, G., Hoch, G., Pernek, M., Preidl, S., Fischer, R., 2025. European forests are under increasing pressure from global change-driven invasions and accelerating epidemics by insects and diseases. Themenh. Waldschutz Im Klimawandel 77, 6–24. https://doi.org/10.5073/JfK.2025.02.02

Hermann, M., Röthlisberger, M., Gessler, A., Rigling, A., Senf, C., Wohlgemuth, T., Wernli, H., 2023. Meteorological history of low-forest-greenness events in Europe in 2002–2022. Biogeosciences 20, 1155–1180. https://doi.org/10.5194/bg-20-1155-2023

Hlásny, T., König, L., Krokene, P., Lindner, M., Montagné-Huck, C., Müller, J., Qin, H., Raffa, K.F., Schelhaas, M.-J., Svoboda, M., Viiri, H., Seidl, R., 2021. Bark Beetle Outbreaks in Europe: State of Knowledge and Ways Forward for Management. Curr. For. Rep. 7, 138–165. https://doi.org/10.1007/s40725-021-00142-x

Jactel, H., Bauhus, J., Boberg, J., Bonal, D., Castagneyrol, B., Gardiner, B., Gonzalez-Olabarria, J.R., Koricheva, J., Meurisse, N., Brockerhoff, E.G., 2017. Tree Diversity Drives Forest Stand Resistance to Natural Disturbances. Curr. For. Rep. 3, 223–243. https://doi.org/10.1007/s40725-017-0064-1

https://doi.org/10.5194/egusphere-2025-6288
Preprint. Discussion started: 19 December 2025

Jaime, L., Batllori, E., Ferretti, M., Lloret, F., 2022. Climatic and stand drivers of forest resistance to recent bark beetle disturbance in European coniferous forests. Glob. Change Biol. 28, 2830–2841. https://doi.org/10.1111/gcb.16106

Jakoby, O., Lischke, H., Wermelinger, B., 2019. Climate change alters elevational phenology patterns of the European spruce bark beetle (Ips typographus). Glob. Change Biol. 25, 4048–4063. https://doi.org/10.1111/gcb.14766

Junttila, S., Blomqvist, M., Laukkanen, V., Heinaro, E., Polvivaara, A., O'Sullivan, H., Yrttimaa, T., Vastaranta, M., Peltola, H., 2024. Significant increase in forest canopy mortality in boreal forests in Southeast Finland. For. Ecol. Manag. 565, 122020. https://doi.org/10.1016/j.foreco.2024.122020

Kärvemo, S., Huo, L., Öhrn, P., Lindberg, E., Persson, H.J., 2023. Different triggers, different stories: Bark-beetle infestation patterns after storm and drought-induced outbreaks. For. Ecol. Manag. 545, 121255. https://doi.org/10.1016/j.foreco.2023.121255

Korhonen K. T., Ahola A. et al. (2021) Forests of Finland 2014–2018 and their development 1921–2018 [WWW Document], n.d. URL https://www.silvafennica.fi/article/10662 (accessed 7.3.25).

Living with bark beetles: impacts, outlook and management options | European Forest Institute [WWW Document], 2019. URL https://efi.int/publications-bank/living-bark-beetles-impacts-outlook-and-management-options (accessed 7.8.25).

Migliavacca, M., Grassi, G., Bastos, A., Ceccherini, G., Ciais, P., Janssens-Maenhout, G., Lugato, E., Mahecha, M.D., Novick, K.A., Peñuelas, J., Pilli, R., Reichstein, M., Avitabile, V., Beck, P.S.A., Barredo, J.I., Forzieri, G., Herold, M., Korosuo, A., Mansuy, N., Mubareka, S., Orth, R., Rougieux, P., Cescatti, A., 2025. Securing the forest carbon sink for the European Union's climate ambition. Nature 643, 1203–1213. https://doi.org/10.1038/s41586-025-08967-3

Mosig, C., Vajna-Jehle, J., Mahecha, M.D., Cheng, Y., Hartmann, H., Montero, D., Junttila, S., Horion, S., Schwenke, M.B., Adu-Bredu, S., Al-Halbouni, D., Allen, M., Altman, J., Angiolini, C., Astrup, R., Barrasso, C., Bartholomeus, H., Brede, B., Buras, A., Carrieri, E., Chirici, G., Cloutier, M., Cushman, K.C., Dalling, J.W., Dempewolf, J., Denter, M., Ecke, S., Eichel, J., Eltner, A., Fabi, M., Fassnacht, F., Feirreira, M.P., Frey, J., Frick, A., Ganz, S., Garbarino, M., García, M., Gassilloud, M., Ghasemi, M., Giannetti, F., Gonzalez, R., Gosper, C., Greinwald, K., Grieve, S., Gutierrez, J.A., Göritz, A., Hajek, P., Hedding, D., Hempel, J., Hernández, M., Heurich, M., Honkavaara, E., Jucker, T., Kalwij, J.M., Khatri-Chhetri, P., Klemmt, H.-J., Koivumäki, N., Korznikov, K., Kruse, S., Krüger, R., Laliberté, E., Langan, L., Latifi, H., Lehmann, J., Li, L., Lines, E., Lopatin, J., Lucieer, A., Ludwig, M., Ludwig, A., Lyytikäinen-Saarenmaa, P., Ma, Q., Marino, G., Maroschek, M., Meloni, F., Menzel, A., Meyer, H., Miraki, M., Moreno-Fernández, D., Muller-Landau, H.C., Mälicke, M., Möhring, J., Müllerova, J., Neumeier, P., Näsi, R., Oppgenoorth, L., Palmer, M., Paul, T., Potts, A., Prober, S., Puliti, S., Pérez-Priego, O., Reudenbach, C., Rossi, C., Ruehr, N.K., Ruiz-Benito, P., Runge, C.M., Scherer-Lorenzen, M., Schiefer, F., Schladebach, J., Schmehl, M.-T., Schwarz, S., Seidl, R., Shafeian, E., Simone, L. de, Sohrabi, H., Sotomayor, L., Sparrow, B., Steer, B.S.C., Stenson, M., Stöckigt, B., Su, Y., Suomalainen, J., Torresani, M., Umlauft, J., Vargas-Ramírez, N., Volpi, M., Vásquez, V., Weinstein, B., Ximena, T.C., Zdunic, K., Zielewska-Büttner, K., Oliveira, R.A. de, Wagtendonk, L. van, Dosky, V. von, Kattenborn, T., 2024. deadtrees.earth - An Open-Access and Interactive Database for Centimeter-Scale Aerial Imagery to Uncover Global Tree Mortality Dynamics. https://doi.org/10.1101/2024.10.18.619094

Nabuurs, G.-J., Lindner, M., Verkerk, P.J., Gunia, K., Deda, P., Michalak, R., Grassi, G., 2013. First signs of carbon sink saturation in European forest biomass. Nat. Clim. Change 3, 792–796. https://doi.org/10.1038/nclimate1853

Network, I.T.M., 2025. Towards a global understanding of tree mortality. New Phytol. 245, 2377–2392. https://doi.org/10.1111/nph.20407

https://doi.org/10.5194/egusphere-2025-6288
Preprint. Discussion started: 19 December 2025

Neuner, S., Albrecht, A., Cullmann, D., Engels, F., Griess, V.C., Hahn, W.A., Hanewinkel, M., Härtl, F., Kölling, C., Staupendahl, K., Knoke, T., 2015. Survival of Norway spruce remains higher in mixed stands under a dryer and warmer climate. Glob. Change Biol. 21, 935–946. https://doi.org/10.1111/gcb.12751

O'Sullivan, M., Sitch, S., Friedlingstein, P., Luijkx, I.T., Peters, W., Rosan, T.M., Arneth, A., Arora, V.K., Chandra, N., Chevallier, F., Ciais, P., Falk, S., Feng, L., Gasser, T., Houghton, R.A., Jain, A.K., Kato, E., Kennedy, D., Knauer, J., McGrath, M.J., Niwa, Y., Palmer, P.I., Patra, P.K., Pongratz, J., Poulter, B., Rödenbeck, C., Schwingshackl, C., Sun, Q., Tian, H., Walker, A.P., Yang, D., Yuan, W., Yue, X., Zaehle, S., 2024. The key role of forest disturbance in reconciling estimates of the northern carbon sink. Commun. Earth Environ. 5, 1–10. https://doi.org/10.1038/s43247-024-01827-4

Pan, Y., Birdsey, R.A., Phillips, O.L., Houghton, R.A., Fang, J., Kauppi, P.E., Keith, H., Kurz, W.A., Ito, A., Lewis, S.L., Nabuurs, G.-J., Shvidenko, A., Hashimoto, S., Lerink, B., Schepaschenko, D., Castanho, A., Murdiyarso, D., 2024. The enduring world forest carbon sink. Nature 631, 563–569. https://doi.org/10.1038/s41586-024-07602-x

Patacca, M., Lindner, M., Lucas-Borja, M.E., Cordonnier, T., Fidej, G., Gardiner, B., Hauf, Y., Jasinevičius, G., Labonne, S., Linkevičius, E., Mahnken, M., Milanovic, S., Nabuurs, G.-J., Nagel, T.A., Nikinmaa, L., Panyatov, M., Bercak, R., Seidl, R., Ostrogović Sever, M.Z., Socha, J., Thom, D., Vuletic, D., Zudin, S., Schelhaas, M.-J., 2023. Significant increase in natural disturbance impacts on European forests since 1950. Glob. Change Biol. 29, 1359–1376. https://doi.org/10.1111/gcb.16531

Pulgarin Diaz J. A., Melin M. et al. (2024) Relationship between stand and landscape attributes and *Ips typographus* salvage loggings in Finland [WWW Document], n.d. URL https://www.silvafennica.fi/article/23069 (accessed 7.3.25).

Raffa, K.F., Aukema, B.H., Bentz, B.J., Carroll, A.L., Hicke, J.A., Turner, M.G., Romme, W.H., 2008. Cross-scale Drivers of Natural Disturbances Prone to Anthropogenic Amplification: The Dynamics of Bark Beetle Eruptions. BioScience 58, 501–517. https://doi.org/10.1641/B580607

Regulation - 2023/839 - EN - EUR-Lex [WWW Document], n.d. URL https://eur-lex.europa.eu/eli/reg/2023/839/oj/eng (accessed 7.8.25).

Regulation - EU - 2024/1991 - EN - EUR-Lex [WWW Document], n.d. URL https://eur-lex.europa.eu/legal-content/EN/TXT/?uri=CELEX%3A32024R1991&qid=1722240349976 (accessed 7.28.25).

Ritter, F., Ciais, P., Senf, C., Santoro, M., Xu, Y., Pelissier-Tanon, A., Schwartz, M., Fayad, I., Carvalhais, N., Brandt, M., Fensholt, R., Besnard, S., Avitabile, V., 2025. Alarming decline in the carbon sink of European forests driven by disturbances. https://doi.org/10.21203/rs.3.rs-3671432/v1

Rizzo, M.L., Székely, G.J., 2016. Energy distance. WIREs Comput. Stat. 8, 27–38. https://doi.org/10.1002/wics.1375

Santoro, M., Cartus, O., 2023. ESA Biomass Climate Change Initiative (Biomass_cci): Global datasets of forest above-ground biomass for the years 2010, 2017, 2018, 2019 and 2020, v4. https://doi.org/10.5285/AF60720C1E404A9E9D2C145D2B2EAD4E

Seidl, R., Donato, D.C., Raffa, K.F., Turner, M.G., 2016. Spatial variability in tree regeneration after wildfire delays and dampens future bark beetle outbreaks. Proc. Natl. Acad. Sci. 113, 13075–13080. https://doi.org/10.1073/pnas.1615263113

Seidl, R., Senf, C., 2024. Changes in planned and unplanned canopy openings are linked in Europe's forests. Nat. Commun. 15, 4741. https://doi.org/10.1038/s41467-024-49116-0

Senf, C., Seidl, R., 2022. Post-disturbance canopy recovery and the resilience of Europe's forests. Glob. Ecol. Biogeogr. 31, 25–36. https://doi.org/10.1111/geb.13406

https://doi.org/10.5194/egusphere-2025-6288
Preprint. Discussion started: 19 December 2025

Senf, C., Seidl, R., 2021. Persistent impacts of the 2018 drought on forest disturbance regimes in Europe. Biogeosciences 18, 5223–5230. https://doi.org/10.5194/bg-18-5223-2021

Senf, C., Seidl, R., 2018. Natural disturbances are spatially diverse but temporally synchronized across temperate forest landscapes in Europe. Glob. Change Biol. 24, 1201–1211. https://doi.org/10.1111/gcb.13897

Senf, C., Seidl, R., Knoke, T., Jucker, T., 2025. Taylor's law predicts unprecedented pulses of forest disturbance under global change. Nat. Commun. 16, 6133. https://doi.org/10.1038/s41467-025-61585-5

Siitonen, J., 2014. *Ips acuminatus* kills pines in southern Finland. Silva Fenn. 48.

Sommerfeld, A., Rammer, W., Heurich, M., Hilmers, T., Müller, J., Seidl, R., 2021. Do bark beetle outbreaks amplify or dampen future bark beetle disturbances in Central Europe? J. Ecol. 109, 737–749. https://doi.org/10.1111/1365-2745.13502

Taylor, L.R., 1961. Aggregation, Variance and the Mean. Nature 189, 732–735. https://doi.org/10.1038/189732a0

Turubanova, S., Potapov, P., Hansen, M.C., Li, X., Tyukavina, A., Pickens, A.H., Hernandez-Serna, A., Arranz, A.P., Guerra-Hernandez, J., Senf, C., Häme, T., Valbuena, R., Eklundh, L., Brovkina, O., Navrátilová, B., Novotný, J., Harris, N., Stolle, F., 2023. Tree canopy extent and height change in Europe, 2001–2021, quantified using Landsat data archive. Remote Sens. Environ. 298, 113797. https://doi.org/10.1016/j.rse.2023.113797

Viana-Soto, A., Senf, C., 2025. The European Forest Disturbance Atlas: a forest disturbance monitoring system using the Landsat archive. Earth Syst. Sci. Data 17, 2373–2404. https://doi.org/10.5194/essd-17-2373-2025

Wermelinger, BeaT., Seifert, MarC., 1999. Temperature-dependent reproduction of the spruce bark beetle Ips typographus, and analysis of the potential population growth. Ecol. Entomol. 24, 103–110. https://doi.org/10.1046/j.1365-2311.1999.00175.x

Weynants, M., Ji, C., Linscheid, N., Weber, U., Mahecha, M.D., Gans, F., 2024. Dheed: an ERA5 based global database of dry and hot extreme events from 1950 to 2022. Earth Syst. Sci. Data Discuss. 1–31. https://doi.org/10.5194/essd-2024-396

Zweifel, R., Pappas, C., Peters, R.L., Babst, F., Balanzategui, D., Basler, D., Bastos, A., Beloiu, M., Buchmann, N., Bose, A.K., Braun, S., Damm, A., D'Odorico, P., Eitel, J.U.H., Etzold, S., Fonti, P., Rouholahnejad Freund, E., Gessler, A., Haeni, M., Hoch, G., Kahmen, A., Körner, C., Krejza, J., Krumm, F., Leuchner, M., Leuschner, C., Lukovic, M., Martínez-Vilalta, J., Matula, R., Meesenburg, H., Meir, P., Plichta, R., Poyatos, R., Rohner, B., Ruehr, N., Salomón, R.L., Scharnweber, T., Schaub, M., Steger, D.N., Steppe, K., Still, C., Stojanović, M., Trotsiuk, V., Vitasse, Y., von Arx, G., Wilmking, M., Zahnd, C., Sterck, F., 2023. Networking the forest infrastructure towards near real-time monitoring – A white paper. Sci. Total Environ. 872, 162167. https://doi.org/10.1016/j.scitotenv.2023.162167